

High Accuracy Planetary Orbit Integration

David M. Hernandez^{1,2★} and Matthew J. Holman¹

¹ *Harvard-Smithsonian Center for Astrophysics, 60 Garden St., MS 51, Cambridge, MA 02138, USA*

28 October 2020

ABSTRACT

We present a new, highly accurate code for planetary orbital dynamics, `EnckeHH`. It solves the Encke equations of motion, which assume perturbed Keplerian orbits. By incorporating numerical techniques, we have made the code follow optimal roundoff error growth for fixed time steps, unlike other codes, such as `IAS15`. In a 10^{12} day integration of the outer Solar System, `EnckeHH` was 3.5 orders of magnitude more accurate than `IAS15` in a fixed time step test.

Key words: methods: numerical—celestial mechanics—planets and satellites: dynamical evolution and stability—galaxies:evolution

1 INTRODUCTION

The problem of predicting the orbital motions of planets has existed since before Newton wrote his universal law of gravitation. Initially, such calculations were done by hand, but now we rely on computers to integrate the n -body equations of motion. Generally, there are two contexts for these computations. In the first case, we are interested in determining precise trajectories over a time scale that is short compared to that of any relevant dynamical chaos (e.g., [Rein et al. 2019b](#)). We assume that the initial conditions and the physical forces are known well enough to support reliable predictions. In the second, the goal is more often to integrate many different initial conditions to study long-term stability, explore the dynamical phase space, or to numerically test analytic theories. For these purposes, speed is at a premium. And it is essential to minimize numerical effects that might mimic physical effects that are not present in the actual system, such as dissipation. There is some overlap, but the distinct demands of these two contexts has resulted in very different numerical algorithms.

The needs of solving for precise trajectories are often satisfied by generic conventional integrators for ordinary differential equations (ODEs). Such integrators do not make assumptions about orbits, and require user input of an acceleration function, and sometimes higher order time derivatives (e.g., [Makino 1991](#)). They can use adaptive steps sizes, which are particularly helpful in scale-free problems like gravity which result in stiff differential equations. Several options exist, and their theory has been widely developed. The Bulirsch–Stoer method ([Press et al. 2002](#); [Bulirsch & Stoer 1964](#)) combines Richardson extrapolation with a simple one-step method like leapfrog. Runge–Kutta methods (RK) are one-step methods that use substeps with predetermined spacings; examples are RADAU in `MERCURY6` ([Chambers 1999](#); [Everhart 1985](#)) and `IAS15` ([Rein & Spiegel 2015](#)). Multistep methods keep

track of previous solution points to better make predictions; examples of these codes are described in [Quinlan & Tremaine \(1990\)](#); [Grazier et al. \(2005\)](#); [Makino \(1991\)](#). Conventional integrators can be made particularly powerful if used in conjunction with well-behaved equations. Regularization techniques remove the singularity of Newtonian gravity through changes of coordinates that result in more slowly varying orbits. For computing near-Earth asteroid dynamics, regularization techniques like `Kunstaanheimo–Stiefel` and `EDROMO` ([Stiefel & Scheifele 1971](#); [Amato et al. 2017](#); [Baù et al. 2014](#)) have been used. The truncation error can be at the machine precision level or lower, making roundoff error the dominant error contribution; thus, some authors ([Rein & Spiegel 2015](#); [Grazier et al. 2005](#); [Hairer et al. 2008](#)) have taken special care to control this error. A curious feature about the methods described above, except for the regularization methods, is that they work for any ODEs, not just those describing planetary motion. Arguably, the most popular of these currently is `IAS15` from [Rein & Spiegel \(2015\)](#).

For the second case in which we need long-term calculations, conventional integrators will fail because they have truncation errors that make calculated orbits useless. However, geometric, and especially symplectic ([Ruth 1983](#); [Channell & Scovel 1990](#)) integrators are suitable. These methods conserve the Poincaré invariants of Hamiltonian dynamics. A limitation of symplectic integrators is they usually require a conservative Hamiltonian. they can also require a very specific form of a Hamiltonian; any deviations from this form may require solving expensive implicit equations which defeat the purpose of constructing these methods for long-term calculations. Their time step usually cannot be a function of the current state in contrast to conventional integrators.

Just as symplectic methods respect Poincaré invariants, other algorithms exploit different “geometric” properties of ODEs, resulting in powerful methods. Examples include symmetric methods ([Hairer et al. 2006](#); [Leimkuhler & Reich 2004](#); [Hernandez & Bertschinger 2018](#)), which exploit the time-

★ Email: dmhernandez@cfa.harvard.edu

symmetry of some problems, projection methods (Hairer et al. 2006; Deng et al. 2020), which force the solution to respect certain conserved quantities, and methods that respect the differentiability and smoothness of Hamiltonians (Hernandez 2019a,b).

Wisdom & Holman (1991) realized that using the averaging principle, which says that high frequency terms can be added or removed from the Hamiltonian governing planetary motion, can be used to write a symplectic map for planetary motion, which is widely known the Wisdom–Holman map (WH). It forms the basis of many calculations of long-term planetary dynamics (Chambers 1999; Duncan et al. 1998; Rein & Tamayo 2015; Rein et al. 2019a; Hernandez & Dehnen 2017). WH built upon a previous asteroidal map (Wisdom 1982, 1983), itself a symplectic integrator (although not called that at the time). WH assumes orbits are perturbations of Keplerian ellipses. So its use is more limited in some ways than the aforementioned conventional methods. For example, it will fail to accurately represent the motion during a close encounter of two planets. Some works have addressed some drawbacks of WH (Chambers 1999; Tsang et al. 2015; Tamayo et al. 2020).

Ideally, we could use conventional integrators to solve equations that exploit the assumption of perturbed Keplerian motion, in the spirit of WH and regularization. But actually, this task was achieved over 150 years ago by Encke, who first wrote his eponymous equations of motion (Encke 1854). Arguably, Encke’s method was more popular in the past, but it was largely replaced by methods that are simpler to program.

In this work, we present a new, highly optimized code to solve Encke’s equations, EnckeHH, where HH stands for Hernandez and Holman. In our code, we have employed a Kepler advancer (Wisdom & Hernandez 2015) with excellent, simple error properties. We have used various numerical techniques to further reduce its error. We show our method follows optimal roundoff error growth, known as Brouwer’s Law (Brouwer 1937); we also say the error is unbiased. This is in contrast to IAS15, which shows biased error growth for fixed time steps. Unlike IAS15, we do not need to rely on adaptive stepping to mitigate error growth. In an integration over 10^{12} days of the outer Solar System, EnckeHH had 3.5 orders of magnitude smaller error than IAS15 for the same step-size. We release our code to the public¹. Instructions on using and running the code on a test problem are also available². Our paper is organized as follows. Section 2 presents the Encke equations of motion. Section 3 presents our optimizations to the method. Section 4 shows short and long-term experiments demonstrating the performance of EnckeHH. We conclude in Section 5.

2 ENCKE METHOD

We describe Encke’s method; a reference is found in Danby (1988). We assume a system with a dominant mass, the star, such that other bodies, the planets, are well described by perturbed Keplerian ellipses. The coordinates and velocities are heliocentric. The planetary positions are written,

$$\mathbf{x}_i = \boldsymbol{\rho}_i + \boldsymbol{\delta}_i, \quad (1)$$

where $\boldsymbol{\rho}_i$ is a Keplerian reference orbit and $\boldsymbol{\delta}_i$ constitutes the perturbations for planet i . The indices are in the range $i \in [1, N]$, where N is the number of planets. The index $i = 0$ is reserved for the star;

its equations of motion are ignored in our code, so all indices in our paper are assumed greater than 0.

The perturbations can be due to any force besides the planet-star point mass Newtonian gravity. The differential equations describing the reference orbits are,

$$\ddot{\boldsymbol{\rho}}_i = -\mu_i \frac{\boldsymbol{\rho}_i}{\rho_i^3}, \quad (2)$$

where $\mu_i = G(m_0 + m_i)$, G is the gravitational constant, and m_0 and m_i are the star and planet mass, respectively. The positions \mathbf{x}_i can be found from integrating,

$$\ddot{\mathbf{x}}_i = -\mu_i \frac{\mathbf{x}_i}{x_i^3} + \mathbf{a}_i(\mathbf{x}, \mathbf{v}, t), \quad (3)$$

where \mathbf{a}_i are accelerations which may depend on the time t . The \mathbf{a}_i can cause the set of ODEs (3) to be coupled. Eqs. (2) and (3) are each initial value problems and require $6N$ initial conditions, with N the number of planets.

We can write an equation for $\boldsymbol{\delta}_i$ from the difference of eqs. (2) and (3):

$$\ddot{\boldsymbol{\delta}}_i = \mu_i \left(\frac{\boldsymbol{\rho}_i}{\rho_i^3} - \frac{\mathbf{x}_i}{x_i^3} \right) + \mathbf{a}_i(\mathbf{x}, \mathbf{v}, t). \quad (4)$$

The quantity in large parentheses is numerically problematic, involving a difference of nearly equal numbers. A useful form is given by,

$$\ddot{\boldsymbol{\delta}}_i = -\frac{\mu_i}{\rho_i^3} \boldsymbol{\delta}_i + \frac{\mu_i}{\rho_i^3} \left(1 - \frac{\rho_i^3}{x_i^3} \right) \mathbf{x}_i + \mathbf{a}_i(\mathbf{x}, \mathbf{v}, t). \quad (5)$$

As written, the quantity in parentheses is still problematic, but it can be recast in a form that avoids the difference of similar quantities (Battin et al. 1987). We first define the auxiliary quantity,

$$q_i = \frac{(\boldsymbol{\delta}_i + 2\boldsymbol{\rho}_i) \cdot \boldsymbol{\delta}_i}{\rho_i^2}. \quad (6)$$

There are other forms of q_i in the literature, but we found this one appealing because it avoids the use of \mathbf{x}_i , whose calculation is prone to roundoff error (see Section 3). Then we define the function,

$$f(q_i) = \left(1 - \frac{\rho_i^3}{x_i^3} \right), \quad (7)$$

which can be rewritten as,

$$f(q_i) = q_i \frac{3 + 3q_i + q_i^2}{(1 + q_i)^{3/2} + (1 + q_i)^3}. \quad (8)$$

The form (8) is the one we use. It can be represented as a series in the small parameter q_i , but we opted for this exact representation. As a demonstration of the importance of properly treating this difference of like quantities, let $\boldsymbol{\rho}_i = (1.0, 0, 0)$ and $\boldsymbol{\delta}_i = (10^{-14}, 0, 0)$. On a machine using double precision arithmetic in IEEE standard, form (7) gives $f(q_i) = 2.997602166487923 \times 10^{-14}$ while form (8) gives a more correct $f(q_i) = 2.99999999999941 \times 10^{-14}$.

The final equations of motion are,

$$\ddot{\boldsymbol{\delta}}_i = -\frac{\mu_i}{\rho_i^3} [\boldsymbol{\delta}_i - f(q_i)\mathbf{x}_i] + \mathbf{a}_i(\mathbf{x}, \mathbf{v}, t), \quad (9)$$

which we call Encke’s equations of motion.

¹ github.com/matthewholman/rebound

² github.com/matthewholman/rebound/tree/master/examples/encke_hh/README.txt

2.1 Calculation of accelerations

As an example for the form of $\mathbf{a}_i(\mathbf{x}, \mathbf{v}, t)$, assume it is due to point mass contributions from the other planets. Let $\mathbf{x}_{ij} = \mathbf{x}_i - \mathbf{x}_j$. Then it takes form,

$$\mathbf{a}_i(\mathbf{x}) = -Gm_j \sum_{j \neq i} \left(\frac{\mathbf{x}_{ij}}{x_{ij}^3} + \frac{\mathbf{x}_j}{x_j^3} \right). \quad (10)$$

Immediately, the $3N$ equations (9) have become coupled. This form of the acceleration is assumed in the remainder of this paper.

3 NUMERICAL IMPLEMENTATION

3.1 Solving the Kepler equation

To implement our Encke method, we need to solve both eqs. (2) and (9). Eq. (2) can be solved as a function of time, and (9) depends on this solution. First, we focus on solving the initial value problem (2). Fortunately, there exist excellent modern methods to solve this such as those in Rein & Tamayo (2015); Wisdom & Hernandez (2015). The Wisdom & Hernandez (2015) solver, `Universal.c`, avoids the Strumpff series expansion used by Rein & Tamayo (2015), in the same way we avoid the series expansion of (8), and in this paper we use a modified `Universal.c`. Our modification is as follows.

When solving for the universal variable s in eq. (35) of Wisdom & Hernandez (2015) we have iterated until convergence. Let $s^{(k)}$ be the value of s after k iterations. Our criteria for convergence is that either $s^{(k)} = s^{(k-1)}$ or $s^{(k)} = s^{(k-2)}$. For the iteration strategy we use a Newton method first. A failsafe is provided by the bisection method. Finally, the timestep is divided if both of these fail. Otherwise, `Universal.c` remains the same. In a typical planetary system problem, bisection is rarely used. For example, when integrating the outer Solar System for 10^7 days using $h = 100$ days, where h is the stepsize, the bisection method was only used 4 times in 8×10^5 calls to the Kepler advancer.

Any update to a reference orbit from the Kepler solver used compensated summation (Kahan 1965; Hairer et al. 2006; Wisdom 2018) to mitigate roundoff error. Compensated summation solves the problem of the precision lost when adding two numbers that are significantly different in order of magnitude by recording the error made after each sum and later compensating for the error.

3.2 Solving the Encke equations of motion

Solving the Encke equations of motion, (9), requires an ODE solver. We have opted for the power series method used by works such as Everhart (1985) and Rein & Spiegel (2015). As shown by Everhart (1974), this series method is equivalent to a Runge–Kutta (RK) method, so in what follows, we will also refer to it as an RK method. This particular RK method is 15th order and uses Gauss–Radau spacings for the substeps. We have built upon code from the Rein & Spiegel (2015) implementation, IAS15. As in earlier works, we used fixed-point iteration to solve for the RK implicit set of equations, with an initial guess obtained from extrapolation.

As an iteration convergence criteria for the RK method, we retained the strict error tolerance from IAS15, which uses the last term in the power series for the acceleration. We have attempted various less strict criteria, which did not work as well, despite δ_i usually being small. As an example, we tried enforcing convergence in \mathbf{x}_i rather than δ_i . In addition, we allow iterations to stop if

the error has grown compared to a previous iteration. This situation occurred rarely. In the same test as in Sec. 3.1, it occurred in 248 steps, or 0.3% of the timesteps.

We have taken care to reduce roundoff error by implementing various numerical techniques—for example, compensated summation again. The additions in (1), (9), and (10) have been performed with compensated summation.

We have used rectification, which is resetting of the reference orbit, once δ_i becomes too large. Specifically, for the rectification criterion we have used,

$$\Delta_i = \frac{\delta_i}{a_i(1-e_i)} > \epsilon, \quad (11)$$

where a_i and e_i are the semi-major axis and eccentricity of the reference orbit, respectively. ϵ is specified by the user, and we set it by default to 0.01. This value was used in tests in this paper. The criteria (11) is not perfect; in particular, a concern is that, especially for large steps, δ_i may become large in the middle of the timestep. However, this was never a problem in our tests. For example, running our Solar System problem for 10^8 days with stepsizes from 0 to 400 days, the condition $|\Delta_i - \epsilon|/\epsilon > 1$ was never satisfied. Using $h = 40$ days, a rectification was performed approximately every 139 steps.

The new orbit is defined by,

$$\begin{aligned} \rho'_i &= \rho_i + \delta_i, \\ \dot{\rho}'_i &= \dot{\rho}_i + \dot{\delta}_i, \\ \delta'_i &= 0, \text{ and} \\ \dot{\delta}'_i &= 0, \end{aligned} \quad (12)$$

where primes indicate new values. If ϵ is too large, the reference orbit is no longer a good approximation and the assumption of δ_i small, made in EnckeHH, breaks down. If ϵ is too small, frequent rectifications occur which slow the code down and increase the number of iterations the RK method needs to converge. This is because the initial guess for the accelerations at the substeps, from extrapolation at the previous step, can no longer be used. For our value of ϵ , this was never a problem. Running the outer Solar System for 10^7 days with $h = 40$ days, we calculate the average number of iterations after a rectification is done, and compare it to the average otherwise. These values are 4.3 and 2.4, respectively. For $h = 400$ days, these values are 7.2 and 6.6, respectively. These differences in iteration number affected computation times in our tests negligibly.

3.3 Other numerical considerations

When designing EnckeHH, there were a number of numerical issues we considered. An incomplete list is given here:

- (i) Our choice of ODE solver for eq. (9) can be improved in future work. For example, this method uses fixed-point iteration to converge to the correct accelerations at 7 substeps, and such an approach requires many iterations for larger steps. However, using a multidimensional Newton iteration (González-Pinto et al. 2001) allows for larger step sizes, which is the strength of the Encke method.
- (ii) Using Gauss–Radau spacings has advantages described in Everhart (1974). However, a disadvantage is that they lead to a mapping that is neither symmetric nor symplectic. This is in contrast to Gauss–Lobatto spacings, which give a symmetric map, or Gauss–Legendre spacings, which lead to a symmetric and symplectic map (Hairer et al. 2006; Faou et al. 2004). If the truncation error

is always guaranteed to be less than the machine precision, the geometric properties of maps with these spacings becomes irrelevant. But if this guarantee is broken for even a tiny fraction of the time, error biases may be introduced. The use of symplectic spacings allowed simplification of the error analysis in [Hairer et al. \(2008\)](#).

- (iii) [Rein & Spiegel \(2015\)](#); [Hairer et al. \(2008\)](#) advocated for defining constants as accurately as possible, but we have not found evidence for special care taken in defining constants in IAS15, and we have not explored this issue ourselves.
- (iv) Adaptive stepping mitigates roundoff error biases to some extent, as correctly claimed by [Rein & Spiegel \(2015\)](#). However, to make a code as unbiased as possible, we focus on behavior using fixed timestep. Adaptive timestepping may not be practical for all problems, for instance, if the information of a reference body is known only at specific time intervals. In addition, adaptive stepping is not a perfect solution for biased errors. Next, there is no reason adaptive stepping should be needed for planetary problems with well-defined timescales that we focus on here, except for extremely eccentric orbits for which $e_i \approx 1$. For such orbits, we have found an adaptive stepping routine useful, which we include in EnckeHH, but we do not focus on it here. Finally, one might argue that introducing an unphysical parameter ϵ to control the adaptive stepsize is unsatisfying. [Rein & Spiegel \(2015\)](#) argue this parameter should be about $\epsilon = 0.01$ but use a default of $\epsilon = 10^{-9}$.

4 NUMERICAL EXPERIMENTS

With EnckeHH, we have been able to produce the most accurate integrations of the outer Solar System that we are aware of.

4.1 Short-term simulations

Our test problem is the Sun plus four outer giant planets. Initial conditions from [Applegate et al. \(1986\)](#) are used. The system of units is au, days, and solar mass. We first run short-term integrations for 5×10^7 days $\approx 11,542P$, where P is the Jupiter period, and compare EnckeHH with IAS15. We use a constant time step, which turns out to be a challenging test. We use the Rebound options,

```
r->heartbeat = heartbeat;
r->force_is_velocity_dependent = 0;
r->integrator = REB_INTEGRATOR_IAS15;
r->gravity = REB_GRAVITY_COMPENSATED;
r->ri_ias15.epsilon = 0; ;
```

Note, we have turned on compensated gravity for IAS15 in an attempt to make the IAS15 integration as accurate as possible (compensated summation is always used in EnckeHH).

In Fig. 1 and 2, we plot the CPU time and energy error as a function of timestep. For steps larger than $h = 400$, the number of RK iterations needed for convergence quickly becomes too large, so that fixed point iteration no longer becomes useful. In Fig. 1, the CPU time for IAS15 is about 32% faster on average, while in Fig. 2, the absolute value of the errors for IAS15 are a median factor of 20 times larger.

In the remaining tests in this paper, we will continue to use the energy error as a metric for how “good” EnckeHH is. We justify this approach by showing the accuracy in phase space for the test problem of Figs. 1 and 2. To measure the accuracy in phase space, we use a reversibility test. Unlike methods like WH, EnckeHH is not formally time-reversible/symmetric ([Hairer et al. 2006](#); [Hernandez & Bertschinger 2018](#)). If we integrate the problem of Fig. 1 and 2 with WH with any step size, reverse the sign

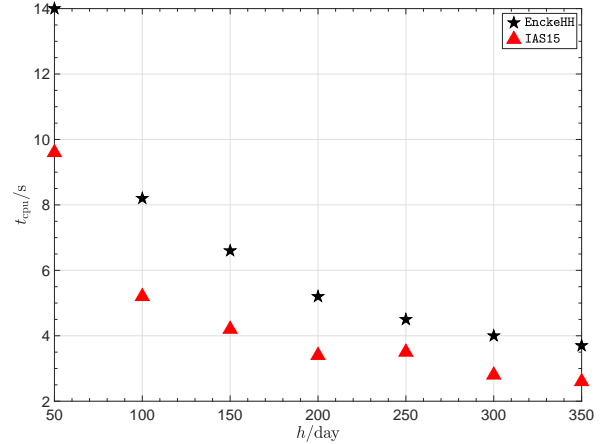


Figure 1. CPU compute time vs timestep for short-term integrations of the outer Solar System for 5×10^7 days. The CPU time for IAS15 is an average of 32% faster than IAS15 in this plot. For steps greater than 400 days, the number of fixed point iterations becomes large.

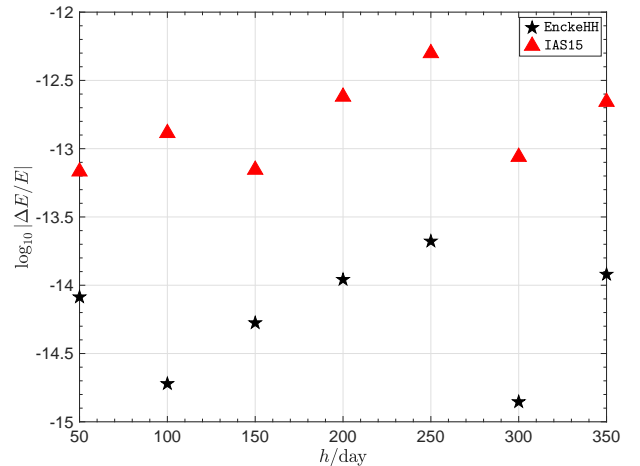


Figure 2. Energy error vs timestep for short-term outer Solar System integrations over 5×10^7 days. The absolute value of the IAS15 errors are a median factor of 20 times larger than the EnckeHH errors.

of velocities, and integrate the same number of steps, WH would exactly recover the initial conditions on an infinitely precise machine, despite possibly large errors in the energy. The same is not true of EnckeHH: if it gives a time-reversible solution, its only because it has solved the phase space from the equations of motion (9) exactly, and thus the energy error is also 0.

In our test, we integrate forward the problem of Figs. 1 and 2, reverse the sign of the time step, and integrate backward. We then calculate the L_2 norm, defined as,

$$L_2 = \sqrt{\sum_i (x_i - x'_i)^2}, \quad (13)$$

where x_i are the initial planetary positions, and x'_i are the final coordinates. In Table 4.1, we show the value of L_2 and the energy error for various step sizes. The energy error is calculated after the for-

h	$\Delta E/E$	L_2
100	5.8×10^{-15}	3.9×10^{-9}
300	2.7×10^{-14}	3.1×10^{-9}
500	3.5×10^{-13}	4.5×10^{-7}
700	5.7×10^{-13}	1.2×10^{-5}
900	-1.9×10^{-10}	2.7×10^{-4}

Table 1. Results of the reversibility test of EnckeHH applied to the test problem of Figs. 1 and 2. The energy error is a rough proxy for the phase space error.

ward integration. We see the energy error is an approximate proxy for L_2 . This justifies our use of energy error as a measure of the “goodness” of EnckeHH. Further work on the relationship between energy error and phase space accuracy was done in Hernandez et al. (2020).

Next, we examine in Fig. 3 the statistical error over time of 1000 nearby initial conditions. The outer Solar System is run for 10^7 days with $h = 40$ days. The IAS15 options remain the same. The initial conditions are generated by displacing Jupiter’s x -position by an amount,

$$\eta = n \times 10^{-14}, \quad (14)$$

where n is an integer such that $n \in [0, 1000)$. Only 125 initial conditions with each method are plotted for clarity of the figure. 100 points are used to plot each curve. The means are indicated with a thick line, while dashed lines indicate sample standard deviations. It is clear already in this short-term integration that IAS15 suffers from a linear bias in its roundoff error. Hairer et al. (2008) suggest that a linear bias can result from constants that are not carefully defined, so this may be an explanation. The error of EnckeHH is dominated by Kepler solver error, which has been investigated carefully and reduced previously (Wisdom & Hernandez 2015). The maximum value of the absolute value of the mean for EnckeHH is $5.8 \times 10^{-16} = 2.6\alpha$, where α is the machine precision, which may indicate a nearly negligible bias. The standard deviation follows Brouwer’s Law and is described by, $\sigma = 5.7 \times 10^{-18} \sqrt{n} + 2.1 \times 10^{-16}$, where $n = t/h$, and $t = 10^7$ days. Thus, the error per timestep is $\approx 0.01\alpha$, so roundoff errors have been clearly suppressed as the errors are committed.

To investigate the statistics further, Fig. 4 plots a histogram of the errors at the last timestep. Normal distributions with the final means and standard deviations have been plotted as well. The errors for both EnckeHH and IAS15 approximately follow normal distributions with sample standard deviations of 3.04×10^{-15} and 3.12×10^{-15} , respectively. By calculating the error in these sample standard deviations, we show in Appendix A that they are consistent.

4.2 Long-term simulations

Finally, we study long-term simulations of the outer Solar System over 10^{12} days $\approx 2.3 \times 10^8 P$, in Fig. 5, where the log of the absolute error is plotted versus time. The same timesteps as in Section 4.1 are used for EnckeHH and IAS15, but we have also calculated $h = 200$ runs with EnckeHH, not shown here, and its roundoff error grew at the same rate. We also plot IAS15 using adaptive stepping as recommended in Rein & Spiegel (2015), using a starting timestep of 40 days, and adaptive step option, `r->ri_ias15.epsilon = 1e-9`.

For a run over 10^8 days, this adaptive stepping yields an average stepsize of $h = 85$ days. For each of the three methods, 1000 logarithmically spaced outputs per run have been plotted and 20 runs

have been performed, by generating initial conditions according to eq. (14) with $n \in [0, 20)$. Mean errors in log space are indicated with solid lines.

Again, a clear linear bias is seen in the IAS15 fixed step case. Adaptive stepping mitigates, but does not eliminate completely, the biased behavior. The EnckeHH behavior appears unbiased with an error that usually remains below that of IAS15, even with adaptive stepping. At the end of the integration, the mean EnckeHH error is $10^{-3.5}$ times that of the IAS15 error with fixed step.

5 CONCLUSIONS

We have presented a code for calculating planetary dynamics orbits with high accuracy. Our code has unbiased roundoff error growth, following Brouwer’s Law. EnckeHH is significantly more accurate than the code IAS15 for fixed timesteps: in integrations of the outer Solar System over 10^{12} days, EnckeHH was 3.5 orders of magnitude more accurate than IAS15 for a timestep. We have improved the error behavior of EnckeHH by using numerical tools such as compensated summation and by being careful with the convergence of the solution of implicit equations, such as the Kepler equation.

While other codes like IAS15 solve generic ODEs, EnckeHH is optimized for planetary orbits and, indeed, any gravitational N -body problem with a dominant central mass. It does not rely on adaptive stepping like IAS15 to mitigate its roundoff error. In our tests, IAS15 was 32% faster than EnckeHH. Our code allows for adaptive stepping, but we did not find this necessary except for orbits that were nearly parabolic.

Many further improvements to EnckeHH are possible. Examples include:

- (i) changing the iteration scheme from fixed point to Newtonian,
- (ii) using different RK spacings with better error properties,
- (iii) modifying the code so that arbitrary forces can be input, and
- (iv) making the code able to handle close encounters by switching to a generic ODE solver when some criteria is satisfied.

6 ACKNOWLEDGEMENTS

We thank Sam Hadden and Matthew Payne for helpful discussions.

7 DATA AVAILABILITY

Our code is released to the public. Instructions on how to use EnckeHH on a test problem are available³.

APPENDIX A: ERROR IN THE SAMPLE STANDARD DEVIATION

We compute the error in the sample standard deviations, s , reported in Section 4.1. For large sample sizes, an unbiased estimator of this error, σ , is found from,

$$\sigma = s \sqrt{e \cdot \left(1 - \frac{1}{n}\right)^{n-1} - 1}, \quad (A1)$$

³ github.com/matthewholman/rebound/tree/master/examples/encke_hh/README.txt

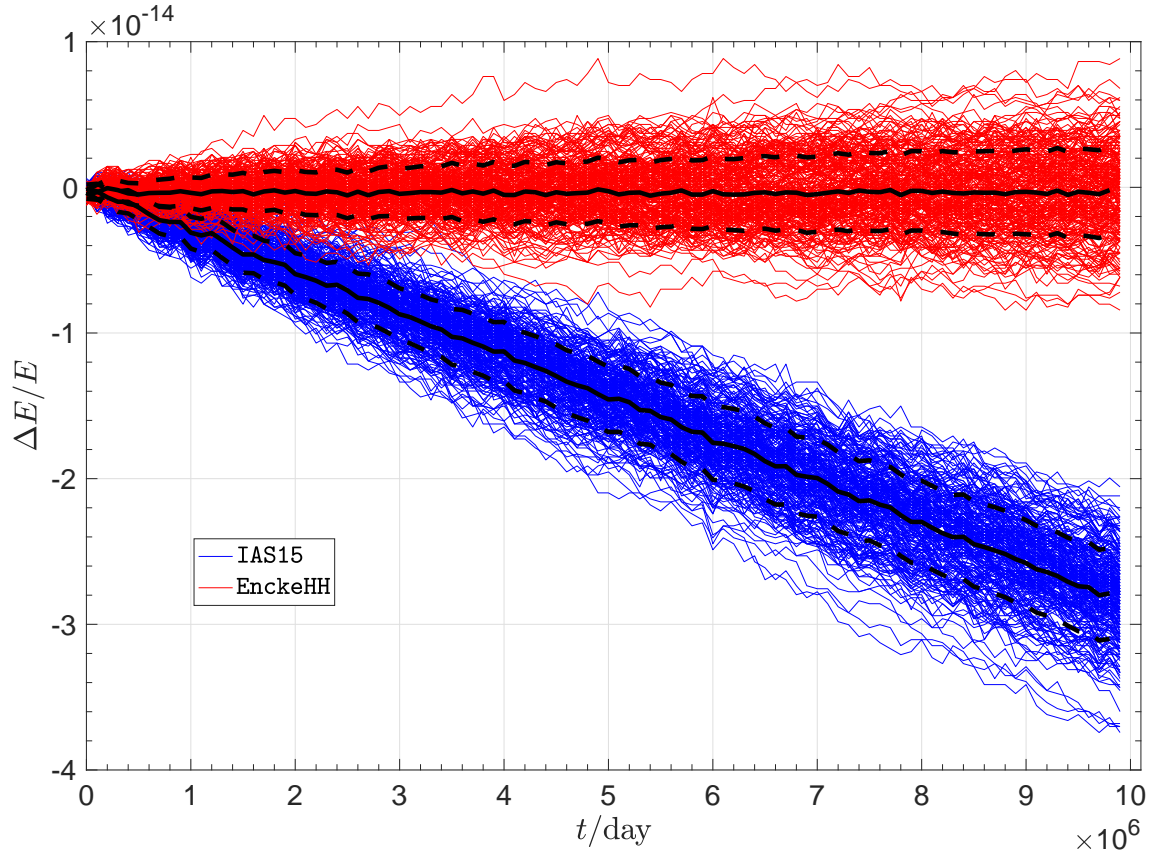


Figure 3. Energy error vs time for 125 outer Solar System initial conditions integrated over 10^7 days, and using $h = 40$ days. The mean and standard deviations have been plotted for 1000 initial conditions. The IAS15 integrations show linear bias while bias has been largely suppressed in the EnckeHH data.

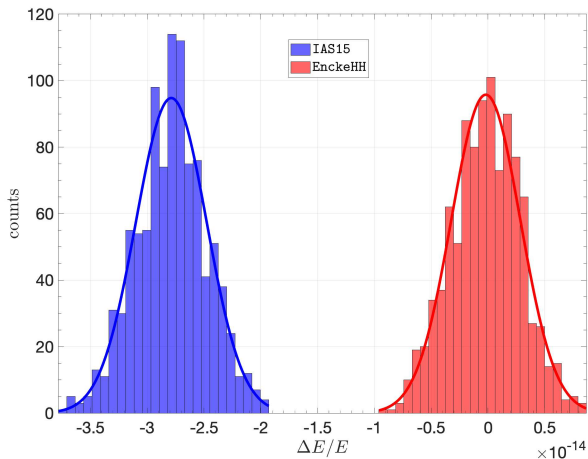


Figure 4. Histogram of the energy errors at the last step of 1000 initial conditions of the outer Solar System, integrated over 10^7 days. The mean and standard deviations in the last time step of Fig. 3 have been used to compute normal curves, which are also plotted. The data are approximately normally distributed, but only the EnckeHH data are approximately centered around 0. More specifically, the IAS15 and EnckeHH means are -2.8×10^{-14} and -1.9×10^{-16} , respectively, while the standard deviations are, 3.12×10^{-15} and 3.04×10^{-15} .

where $n = 1000$ is the sample size. Using the s from Section 4.1, we find $\sigma = 6.8 \times 10^{-17}$ and $\sigma = 7.0 \times 10^{-17}$ for EnckeHH and IAS15, respectively. This implies the two s are consistent.

REFERENCES

- Amato D., Bau G., Bombardelli C., 2017, *Monthly Notices of the Royal Astronomical Society*, 470, 2079
- Applegate J. H., Douglas M. R., Gursel Y., Sussman G. J., Wisdom J., 1986, *AJ*, 92, 176
- Battin R., of Aeronautics A. I., *Astronautics 1987, An Introduction to the Mathematics and Methods of Astrodynamics*. AIAA Textbook Series, American Institute of Aeronautics and Astronautics
- Bañ G., Urrutxua H., Pelaez J., 2014, *Adv. Astronaut. Sci.*, 152, 379
- Brouwer D., 1937, *AJ*, 46, 149
- Bulirsch R., Stoer J., 1964, *Numerische Mathematik*, 6, 413
- Chambers J. E., 1999, *MNRAS*, 304, 793
- Channell P. J., Scovel C., 1990, *Nonlinearity*, 3, 231
- Danby J. M. A., 1988, *Fundamentals of celestial mechanics*, 2nd rev. and enl. edn. Willmann-Bell, Richmond, Va., U.S.A.
- Deng C., Wu X., Liang E., 2020, *Monthly Notices of the Royal Astronomical Society*, 496, 2946
- Duncan M. J., Levison H. F., Lee M. H., 1998, *AJ*, 116, 2067
- Encke J., 1854, *Berliner Astronomisches Jahrbuch für 1857*, pp 319–397
- Everhart E., 1974, *Celestial Mechanics*, 10, 35
- Everhart E., 1985, in Carusi A., Valsecchi G. B., eds, *Dynamics of Comets: Their Origin and Evolution*, Proceedings of IAU Colloq. 83, held in

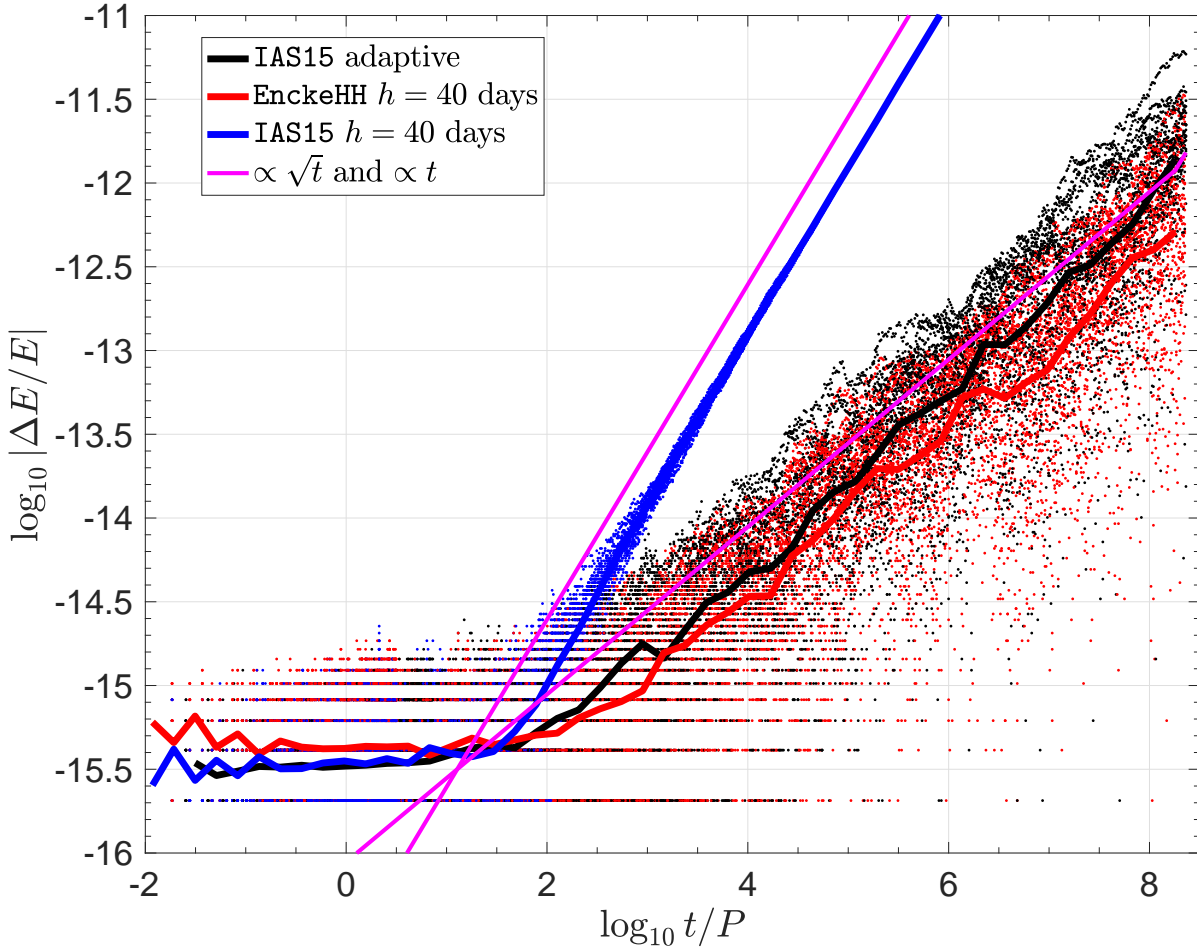


Figure 5. 20 integrations from Fig. 3 are extended to 10^{12} days. We have also used IAS15 with its recommended adaptive stepping parameter $\epsilon = 10^{-9}$. 1000 points are plotted per integration. A mean in log space is indicated with thick lines. The linear bias in the fixed step IAS15 case persists. Its bias is mitigated, but not eliminated, when adaptive stepping is used. The error for EnckeHH usually remains below the IAS15 error.

Rome, Italy, June 11-15, 1984. Edited by Andrea Carusi and Giovanni B. Valsecchi. Dordrecht: Reidel, Astrophysics and Space Science Library. Volume 115, 1985, p.185. p. 185

Faou E., Hairer E., Pham T.-L., 2004, *BIT Numerical Mathematics*, 44, 699

González-Pinto S., Pérez-Rodríguez S., Montijano J., 2001, *Computers & Mathematics with Applications*, 41, 1009

Grazier K. R., Newman W. I., Hyman J. M., Sharp P. W., Goldstein D. J., 2005, in May R., Roberts A. J., eds, Vol. 46, Proc. of 12th Computational Techniques and Applications Conference CTAC-2004. pp C786–C804

Hairer E., Lubich C., Wanner G., 2006, Geometrical Numerical Integration, 2nd edn. Springer Verlag, Berlin

Hairer E., McLachlan R., Razakariyony A., 2008, *BIT*, 48, 231

Hernandez D. M., 2019a, *MNRAS*, 486, 5231

Hernandez D. M., 2019b, *MNRAS*, 490, 4175

Hernandez D. M., Bertschinger E., 2018, *MNRAS*, 475, 5570

Hernandez D. M., Dehnen W., 2017, *MNRAS*, 468, 2614

Hernandez D. M., Hadden S., Makino J., 2020, *MNRAS*, 493, 1913

Kahan W., 1965, *Commun. ACM*, 8, 40

Leimkuhler B., Reich S., 2004, Simulating Hamiltonian Dynamics. Cambridge University Press

Makino J., 1991, *ApJ*, 369, 200

Press W. H., Teukolsky S. A., Vetterling W. T., Flannery B. P., 2002, Numerical recipes in C++ : the art of scientific computing

Quinlan G. D., Tremaine S., 1990, *AJ*, 100, 1694

Rein H., Spiegel D. S., 2015, *MNRAS*, 446, 1424

Rein H., Tamayo D., 2015, *MNRAS*, 452, 376

Rein H., et al., 2019a, *MNRAS*, 485, 5490

Rein H., Brown G., Tamayo D., 2019b, *MNRAS*, 490, 5122

Ruth R. D., 1983, *IEEE Transactions on Nuclear Science*, 30, 2669

Stiefel E., Scheifele G., 1971.

Tamayo D., Rein H., Shi P., Hernandez D. M., 2020, *MNRAS*, 491, 2885

Tsang D., Galley C. R., Stein L. C., Turner A., 2015, *ApJ*, 809, L9

Wisdom J., 1982, *AJ*, 87, 577

Wisdom J., 1983, *Icarus*, 56, 51

Wisdom J., 2018, *MNRAS*, 474, 3273

Wisdom J., Hernandez D. M., 2015, *MNRAS*, 453, 3015

Wisdom J., Holman M., 1991, *AJ*, 102, 1528